

END-TO-END ZERO-SHOT VOICE CONVERSION WITH LOCATION-VARIABLE CONVOLUTIONS

Wonjune Kang^{1,2}, Mark Hasegawa-Johnson³, Deb Roy^{1,2}

¹MIT Center for Constructive Communication ²MIT Media Lab
³University of Illinois at Urbana-Champaign

ABSTRACT

Zero-shot voice conversion is becoming an increasingly popular research direction, as it promises the ability to transform speech to match the vocal identity of any speaker. However, relatively little work has been done on end-to-end methods for this task, which are appealing because they remove the need for a separate vocoder to generate audio from intermediate features. In this work, we propose LVC-VC, an end-to-end zero-shot voice conversion model that uses location-variable convolutions (LVCs) to jointly model the conversion and speech synthesis processes with a small number of parameters. LVC-VC utilizes carefully designed input features that have disentangled content and speaker style information, and the neural vocoder-like architecture learns to combine them to perform voice conversion while simultaneously synthesizing audio. Experiments show that our model achieves competitive or better voice conversion performance compared to several baselines while maintaining intelligibility particularly well.

Index Terms— Voice conversion, style transfer, speech synthesis, location-variable convolutions

1. INTRODUCTION

Voice conversion (VC) is the task of transforming a voice to sound like that of another person without changing the linguistic or prosodic content in the original speech. It has many practical applications, such as voice anonymization, communication aids for the speech-impaired, and voice dubbing, which have contributed to its increasing popularity as a research direction in recent years. Advances in deep learning have had a significant impact on voice conversion research, allowing VC systems to achieve significant improvements in terms of voice quality and similarity to the target speaker, especially in the non-parallel data setting [1, 2, 3].

Recently, attention has been shifting to zero-shot VC, a more difficult setting in which conversion is applied to new speakers that were previously unseen during training. A key aspect of zero-shot VC is the disentanglement, separation, and recombination of the content and speaker information in input and target speakers' utterances. Traditionally, this decomposition and recombination are performed on intermediate representations such as mel spectrograms. This is followed by a vocoding step to convert these representations into time-domain audio. However, these approaches necessitate sequential training of each stage using different types of supervision and criteria, leaving the door open for weaknesses in any individual module to contribute to weaknesses in the overall system. Furthermore, these approaches are not able to take advantage of the benefits of data-driven end-to-end learning, which has the advantages of simplicity, elegance, and high performance. Despite this, relatively little work has been done on end-to-end methods for voice conversion.

In this work, we introduce Location-Variable Convolution-based Voice Conversion (LVC-VC), a model for performing end-to-end zero-shot voice conversion that is based on the architecture of a neural vocoder. LVC-VC utilizes location-variable convolutions (LVCs) [4] to efficiently model the time-dependent features that arise in speech with a compact model size. It takes a set of carefully designed input features that have disentangled content and speaker style information, and the vocoder-like architecture learns to combine these features to perform voice conversion while simultaneously synthesizing audio. This significantly streamlines the model's structure and removes the difficult task of teaching the model to perform disentangled representation learning. Experiments demonstrate that LVC-VC achieves competitive or better performance compared to several baselines despite having a significantly smaller number of parameters. Additionally, it is able to maintain the clarity and intelligibility of transformed speech particularly well. This contrasts with other baselines, which we find to exhibit a trade-off between maintaining audio quality/intelligibility and accurate voice style transfer.¹

2. BACKGROUND AND RELATED WORK

Most zero-shot VC models trained on non-parallel data use a self-supervised learning strategy with a reconstruction-based loss. The idea is to decompose a given training utterance's speaker and content information into separate embeddings, and then recombine them using a decoder to reconstruct the original signal. At inference time, conversion is performed by combining the content embedding from a source utterance with the speaker embedding from a target utterance.

One of the first zero-shot voice conversion methods was AutoVC [5], an autoencoder-based model that combined a pre-trained speaker encoder with dimensionality bottleneck layers to disentangle content and speaker information. AutoVC has served as the base model for a range of improvements, such as the addition of fundamental frequency (F0) information [6], mutual information-based disentangled representation learning [7], and adversarial voice style mixup [8]. Other approaches have used techniques such as adaptive instance normalization [9] and activation function guidance [10] to disentangle the content and speaker information in speech. All of the aforementioned methods produce spectrograms, which necessitate that a separate vocoder be part of the overall system in order to synthesize time-domain audio.

Relatively few models have been proposed that can perform end-to-end voice conversion. Blow [11] is a normalizing flow network for non-parallel raw-audio voice conversion. However, it is not able to perform zero-shot conversion, and like many other flow-based networks, it has a very large number of parameters. NVC-Net [12] is a GAN-based zero-shot model that performs conversion directly on

¹Audio samples are available online on our demo page: <https://lvc-vc.github.io/lvc-vc-demo/>

raw audio waveforms. Conceptually, LVC-VC shares some similarities with HiFi-VC [13] and NANSY [14]. HiFi-VC is an end-to-end VC model that uses linguistic, F0, and speaker features as inputs to a conditioned HiFi-GAN [15] decoder, thereby directly synthesizing converted audio. NANSY is a non-end-to-end neural analysis and synthesis framework that uses various input features along with information perturbation-based training to flexibly control speech attributes. However, both of these methods use representations from large pre-trained ASR models for their linguistic input features (Conformer [16] and XLSR-53 [17], respectively), resulting in extremely large model sizes with hundreds of millions of parameters. In contrast, LVC-VC has a significantly smaller number of parameters and uses input features that are much simpler to compute.

3. LVC-VC: LOCATION-VARIABLE CONVOLUTION-BASED VOICE CONVERSION

3.1. Input features

Content. The primary content feature used in LVC-VC is grounded in the source-filter model of speech production, in which the excitation of a speaker’s vocal cords (the source) is convolved with a representation of the vocal tract (the filter) [18]. Here, we consider the excitation to contain the speaker information of an utterance and the vocal tract to contain the content information. Thus, separating the source and filter components by performing deconvolution in the cepstral domain allows us to disentangle speaker and content information to a large extent. Note that the filter actually still contains some speaker information even after deconvolution; in Section 3.3, we describe a training strategy to deal with this issue.

Formally, let a source utterance in the time domain be \mathbf{x} and its log-mel spectrogram be \mathbf{X} . We convert \mathbf{X} to the cepstral domain, perform low-quefrency liftering, and re-convert back to the spectral domain to obtain the spectral envelope of the utterance \mathbf{H} , which serves as the primary content feature for the model. In our experiments, \mathbf{X} is an 80-dimensional log-mel spectrogram computed using a 1024 point Fourier transform, with a Hann window of size 1024 and hop length of size 256. To obtain \mathbf{H} , we take the 20 lowest quefrency coefficients for low-quefrency liftering.

We also use the normalized F0 contour of \mathbf{x} as an additional content-related feature. Specifically, we use the per-frame normalized quantized log F0 \mathbf{p}_{norm} , that was introduced previously in [6]. When extracting the F0, we use the same analysis window and hop sizes as when computing \mathbf{X} to ensure that the number of extracted F0 frames matches up with the number of spectrogram frames.

Speaker. We use speaker embeddings extracted from a pre-trained encoder E_s ; the details of E_s are described more in-depth in Section 3.2. For an utterance \mathbf{x} , its speaker embedding is thus: $s = E_s(\mathbf{x})$.

We also use the quantized median log F0 of a speaker as an additional feature. We first extract the log F0 from all of a speaker’s voiced speech and obtain the median. Then, we quantize the range $\log(65.4)$ Hz to $\log(523.3)$ Hz (corresponding to the notes ‘C2’ and ‘C5’) into 64 bins and one-hot encode the median log F0 value; any values outside the quantized range are clipped. This results in a 64-dimensional vector m that encodes the speaker’s F0 information.

3.2. Model architecture

LVC-VC consists of a generator G , a speaker encoder E_s , and a set of discriminators D for GAN-based training.

Generator. The generator G is a fully convolutional neural network that is based on UnivNet-c16 [19], with a channel size of 16 in each of its convolutional layers. Fig. 1 shows a diagram of the overall

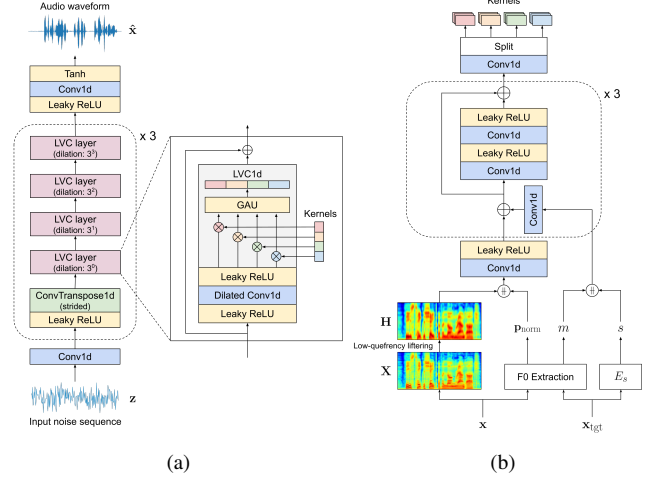


Fig. 1: Overall LVC-VC architecture. (a) Generator. (b) Kernel predictor network for LVC layers. \oplus denotes stacking/concatenation.

architecture. G takes random noise \mathbf{z} as an input sequence and the content and speaker features described in Section 3.1 as conditions, and outputs a raw audio waveform $\hat{\mathbf{x}}$. Its main body consists of a series of 1D transposed convolutions to upsample \mathbf{z} , which has the same length as the content feature \mathbf{H} . In our experiments, spectrograms are at a $256 \times$ lower resolution compared to raw audio. Therefore, there are three transposed convolutions with upsampling factors of $8 \times$, $8 \times$, and $4 \times$ to perform the total $256 \times$ upsampling.

Each transposed convolution is followed by a stack of four residual blocks, each of which consists of a dilated 1D convolution, a 1D location-variable convolution (LVC), and a gated activation unit (GAU). The four dilated convolutions in each stack have dilation factors of $[1, 3, 9, 27]$. Leaky ReLU with $\alpha = 0.2$ is used as the activation function. The LVC kernels are determined by kernel predictor networks that use the conditioning features \mathbf{H} , \mathbf{p}_{norm} , s , and m to simultaneously predict the kernels for all of the LVCs in the stack that they are associated with. The output waveform is thus:

$$\hat{\mathbf{x}} = G(\mathbf{z}, \mathbf{H}, \mathbf{p}_{\text{norm}}, s, m).$$

Speaker encoder. For the speaker encoder E_s , we use the Fast ResNet-34 speaker recognition model from [20]. The model was pre-trained on the development set of the VoxCeleb2 dataset [21] and uses self-attentive pooling to aggregate frame-level features into an utterance-level representation.

Discriminators. LVC-VC uses two discriminators for GAN-based training: a multi-resolution spectrogram discriminator (MRSD) [19] and a multi-period waveform discriminator (MPWD) [15].

The MRSD is a mixture of M sub-discriminators that evaluates a synthesized waveform at multiple frequency resolution scales using short-time Fourier transform (STFT) parameter sets $\{\mathbf{F}^T_m(\cdot)\}_{m=1}^M$. Each parameter set consists of: (# of Fourier transform points, window length (seconds), hop length (seconds)). Formally, the MRSD computes: $\{\mathbf{s}_m = |\mathbf{F}^T_m(\mathbf{x})|, \hat{\mathbf{s}}_m = |\mathbf{F}^T_m(\hat{\mathbf{x}})|\}_{m=1}^M$. In our experiments, $M = 3$ and the parameter sets for the sub-discriminators were $[(512, 0.025, 0.005), (1024, 0.05, 0.01), (256, 0.01, 0.002)]$.

The MPWD is also a mixture of sub-discriminators, each of which takes as input equally spaced samples of an audio waveform at a different period p and evaluates whether it is real or not. The periods are set to the prime numbers $[2, 3, 5, 7, 11]$ in order to avoid overlaps in analysis between the sub-discriminators as much as possible.

Table 1: Model sizes and voice conversion evaluation results on the three conversion settings. We include 95% confidence intervals for MOS. Bold and underlined values indicate the best and second best scores in a given metric, respectively.

Model	Size	Seen-to-Seen				Unseen-to-Seen				Unseen-to-Unseen			
		MOS	Sim	CER	EER	MOS	Sim	CER	EER	MOS	Sim	CER	EER
Ground Truth	–	4.61 ± 0.11	91.88	3.81	0.00	4.74 ± 0.08	95.63	2.93	0.00	4.62 ± 0.11	92.50	3.58	0.00
UnivNet	–	4.33 ± 0.12	90.63	4.97	5.00	4.51 ± 0.11	97.50	3.59	0.00	4.58 ± 0.10	92.50	4.68	0.00
LVC-VC	5.97M	<u>3.54 ± 0.17</u>	51.88	11.00	<u>17.50</u>	<u>3.51 ± 0.18</u>	43.75	7.03	<u>20.00</u>	3.24 ± 0.18	38.75	8.29	26.25
AdaIN-VC	4.89M	2.35 ± 0.16	<u>63.75</u>	22.78	28.75	2.57 ± 0.17	<u>53.13</u>	16.41	36.25	2.41 ± 0.16	49.38	20.60	35.00
AGAIN-VC	7.93M	2.13 ± 0.16	48.75	25.12	18.75	2.39 ± 0.16	46.25	23.94	31.25	2.26 ± 0.15	<u>42.50</u>	25.79	<u>31.25</u>
AutoVC	40.68M	3.84 ± 0.15	30.63	<u>11.15</u>	30.00	3.71 ± 0.16	31.88	10.65	26.25	3.61 ± 0.17	<u>13.13</u>	<u>12.07</u>	63.75
AutoVC-F0	41.21M	3.44 ± 0.16	32.50	12.53	28.75	3.39 ± 0.16	37.50	<u>10.54</u>	32.50	<u>3.31 ± 0.17</u>	20.00	14.20	65.00
Blow	62.11M	1.78 ± 0.15	29.38	18.33	52.50	–	–	–	–	–	–	–	–
NVC-Net	15.13M	2.96 ± 0.19	76.88	31.46	12.50	3.14 ± 0.19	66.25	26.91	11.25	3.10 ± 0.20	40.00	26.27	37.50

3.3. Training

Self-reconstruction. LVC-VC is trained primarily using a self-reconstruction paradigm, where the content and speaker features from training utterances are used to reconstruct the original audio.

Recall that the content feature \mathbf{H} still contains some amount of speaker information. This residual information could leak into the synthesized audio at inference time, resulting in poor conversion performance. To prevent this from happening, we warp \mathbf{H} by stretching or compressing it along the frequency axis during training; we denote the warped version \mathbf{H}' . This removes most of the residual speaker information in \mathbf{H} while still preserving its content information. For each sample, the warping factor is randomly chosen from a uniform distribution over $[0.85, 1.15]$. For speaker embeddings, rather than using the embedding extracted directly from an utterance, we sample an embedding s' from a GMM with 1 component that we fit on the corresponding speaker’s training utterances. This means that a similar, but different embedding is used to reconstruct an utterance every time, which helps the model generalize better to unseen speakers.

Formally, let a training utterance be \mathbf{x} and the associated features be $\mathbf{H}', \mathbf{p}_{\text{norm}}, s', m$. Then, the reconstructed output is $\hat{\mathbf{x}} = G(\mathbf{z}, \mathbf{H}', \mathbf{p}_{\text{norm}}, s', m)$. In addition to the GAN losses from the discriminators described above, we also use multi-resolution STFT loss [22]. The full auxiliary loss \mathcal{L}_{aux} , which is comprised of the spectral convergence loss \mathcal{L}_{sc} and log STFT magnitude loss \mathcal{L}_{mag} , is:

$$\mathcal{L}_{\text{sc}}(\mathbf{s}, \hat{\mathbf{s}}) = \frac{\|\mathbf{s} - \hat{\mathbf{s}}\|_F}{\|\mathbf{s}\|_F}, \quad \mathcal{L}_{\text{mag}}(\mathbf{s}, \hat{\mathbf{s}}) = \frac{1}{N} \|\log \mathbf{s} - \log \hat{\mathbf{s}}\|_1,$$

$$\mathcal{L}_{\text{aux}}(\mathbf{x}, \hat{\mathbf{x}}) = \frac{1}{M} \sum_{m=1}^M \mathbb{E}_{\mathbf{x}, \hat{\mathbf{x}}} [\mathcal{L}_{\text{sc}}(\mathbf{s}_m, \hat{\mathbf{s}}_m) + \mathcal{L}_{\text{mag}}(\mathbf{s}_m, \hat{\mathbf{s}}_m)].$$

Here, N denotes the number of spectrogram frames and M is the number of MRSD sub-discriminators. \mathbf{s} and $\hat{\mathbf{s}}$ are defined as in Section 3.2, and each m -th \mathcal{L}_{sc} and \mathcal{L}_{mag} reuse \mathbf{s}_m and $\hat{\mathbf{s}}_m$ from the m -th MRSD sub-discriminator.

Speaker similarity. We utilize a speaker similarity criterion (SSC) in order to induce LVC-VC to generate audio that more closely matches the characteristics of the target speaker. Let a given utterance for self-reconstruction be \mathbf{x}_0 and its associated features be $(\mathbf{H}_0, \mathbf{p}_{\text{norm},0}, s_0, m_0)$. For each training sample, we sample N utterances from different speakers $\mathbf{x}_1, \dots, \mathbf{x}_N$ with content features $(\mathbf{H}_n, \mathbf{p}_{\text{norm},n})$, $\forall n \in [1, \dots, N]$. Then, the SSC loss \mathcal{L}_{ssc} is:

$$\hat{\mathbf{x}}_{n \rightarrow 0} = G(\mathbf{z}, \mathbf{H}_n, \mathbf{p}_{\text{norm},n}, s'_0, m_0),$$

$$\mathcal{L}_{\text{ssc}} = \frac{1}{N} \sum_{n=1}^N \cos(E_s(\hat{\mathbf{x}}_{n \rightarrow 0}, s'_0)),$$

where $\cos(x_1, x_2)$ denotes the cosine similarity between x_1 and x_2 .

Overall criteria. During training, we keep the weights of E_s fixed and only update G and D . The overall generator and discriminator losses follow the least-squares GAN objective functions [23]:

$$\mathcal{L}_G = \frac{1}{K} \sum_{k=1}^K \mathbb{E}_{\mathbf{z}, \mathbf{c}} [(D_k(G(\mathbf{x}')) - 1)^2] + \lambda_{\text{aux}} \mathcal{L}_{\text{aux}}(\mathbf{x}, G(\mathbf{x}')) + \lambda_{\text{ssc}} \mathcal{L}_{\text{ssc}},$$

$$\mathcal{L}_D = \frac{1}{K} \sum_{k=1}^K (\mathbb{E}_{\mathbf{x}} [(D_k(\mathbf{x}) - 1)^2] + \mathbb{E}_{\mathbf{z}, \mathbf{c}} [D_k(G(\mathbf{x}'))^2]),$$

where we abbreviate $G(\mathbf{z}, \mathbf{H}', \mathbf{p}_{\text{norm}}, s', m)$ to $G(\mathbf{x}')$ for conciseness. K denotes the number of all sub-discriminators across the MRSD and MPWD, and D_k denotes the k -th sub-discriminator across all sub-discriminators. λ_{aux} and λ_{ssc} are weighting factors that balance the contributions of the auxiliary loss and SSC loss, respectively.

3.4. Inference

Given source utterance \mathbf{x}_{src} with content features $(\mathbf{H}_{\text{src}}, \mathbf{p}_{\text{norm},\text{src}})$ and target utterance \mathbf{x}_{tgt} with speaker features $(s_{\text{tgt}}, m_{\text{tgt}})$, LVC-VC produces the converted utterance $\hat{\mathbf{x}}_{\text{src} \rightarrow \text{tgt}}$ by:

$$\hat{\mathbf{x}}_{\text{src} \rightarrow \text{tgt}} = G(\mathbf{z}, \mathbf{H}_{\text{src}}, \mathbf{p}_{\text{norm},\text{src}}, s_{\text{tgt}}, m_{\text{tgt}}).$$

4. EXPERIMENTS

4.1. Configurations

We used the VCTK Corpus [24] for training and evaluation. All audio was resampled to 16 kHz. We randomly partitioned the data into 99 “seen” speakers and 10 “unseen” speakers, and the seen speakers’ utterances were further split into train and test sets in a 9:1 ratio. Only utterances from the seen speakers’ train set were used for training.

Training was done on four NVIDIA GTX 1080 Ti GPUs. We used the AdamW optimizer [25] with learning rate $1\text{e-}4$ and $\beta_1 = 0.5$, $\beta_2 = 0.9$. For the SSC loss, we set $N = 8$. Following [19], we set $\lambda_{\text{aux}} = 2.5$, and we empirically set $\lambda_{\text{ssc}} = 0.9$. LVC-VC was trained with only self-reconstructive loss using a batch size of 32 for 1.8M iterations. Then, we halved the learning rate to $5\text{e-}5$ and continued training with the SSC loss included for 5,000 more iterations, using a decreased batch size of 16 due to GPU memory constraints. This strategy ensured that the model first learned to produce high-quality audio before being guided to perform better voice conversion without compromising audio quality. λ_{ssc} was linearly annealed from 0 to its final value for the first 2,000 steps in which the SSC loss was used.

To evaluate, we conducted subjective listening tests for naturalness and speaker similarity on Amazon Mechanical Turk (MTurk). For naturalness, subjects provided a mean opinion score (MOS) on a scale from 1 to 5. For similarity, we used the binary “same/different”

Table 2: Unseen-to-unseen voice conversion evaluation results for various ablations of LVC-VC.

Model	CER	EER	NISQA
LVC-VC	8.29	26.25	3.50 ± 0.13
w/o GMM embeddings	11.11	25.00	2.89 ± 0.14
w/o SSC loss	6.64	68.75	3.83 ± 0.13
w/o warping \mathbf{H}	7.39	51.25	3.62 ± 0.17
w/o \mathbf{p}_{norm}	8.60	32.50	3.36 ± 0.18
w/o m	9.90	28.75	3.47 ± 0.14

metric from [26]. We also utilized two objective metrics: character error rate (CER) on automatic speech recognition (ASR) and equal error rate (EER) on automatic speaker verification (ASV). For ASR, we used a pre-trained wav2vec 2.0 BASE model [27] from the Hugging Face Transformers library [28]. For ASV, we used a ResNet-34-based model [29] that uses attentive statistics pooling to aggregate temporal frames and was trained on the development set of VoxCeleb2.

We considered three source-to-target speaker conversion settings: seen-to-seen (s2s), unseen-to-seen (u2s), and unseen-to-unseen (u2u). For each setting, we evaluated conversions from 80 utterance pairs, each of which was rated by two annotators on MTurk.

4.2. Results

We compared LVC-VC with AdaIN-VC [9], AGAIN-VC [10], AutoVC [5], AutoVC-F0 [6], Blow [11], and NVC-Net [12]. All models were trained from scratch on the same data as LVC-VC. For a fair comparison, models generating spectrograms were trained using the same spectrogram configuration as LVC-VC, and all time-domain audio was synthesized using a UnivNet-c16 vocoder [19] that was trained on the 99 seen speakers from the VCTK dataset as well as the *train-clean-360* split of the LibriTTS dataset [30].

Table 1 shows the scores for each model on the three conversion settings. We found that most of the baselines either perform voice style transfer (VST) well but produce less natural or intelligible audio (AdaIN-VC, AGAIN-VC, NVC-Net), or produce natural and intelligible audio but do not perform VST well (AutoVC, AutoVC-F0). In other words, there is a trade-off between audio quality and VST performance. LVC-VC manages this trade-off much better than the other models. Although it does not quite achieve the best MOS or Similarity, it is competitive with the other best models in these metrics and arguably achieves the most balanced performance. It also obtains the lowest CER, especially in the u2s and u2u settings, demonstrating that it maintains intelligibility particularly well. Notably, LVC-VC achieves its performance with a compact model size; it has the second smallest number of parameters among all the models we tested.

4.3. Ablation studies

We conducted ablation studies on various training strategies and input features used in LVC-VC; the results are shown in Table 2. For brevity and convenience, we only report scores from objective metrics in the u2u setting. As a proxy measure for subjective MOS, we used NISQA [31], which estimates an utterance’s MOS for audio quality on a scale from 1 to 5. We found that each of the ablated components contributed meaningfully to the model’s performance. Training on fixed speaker embeddings instead of sampling from GMMs caused audio quality to degrade, suggesting that training on more diverse embeddings helps the model generalize better to new speakers. Training without SSC loss or without warping \mathbf{H} caused VST performance to decrease, showing the importance of explicitly guiding the model to perform conversion rather than only relying on self-reconstructive training, as well as perturbing the source speaker information in \mathbf{H} . Finally, \mathbf{p}_{norm} and m contributed to general performance gains in all metrics.

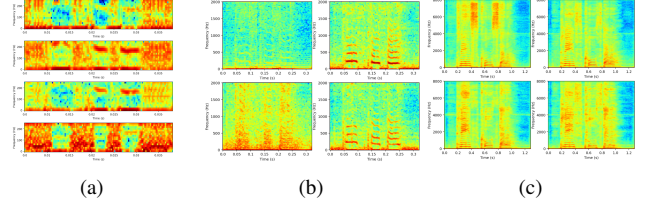


Fig. 2: Results of computing the STFT on outputs of the (a) first, (b) second, and (c) third transposed convolutional stacks of LVC-VC. For brevity, we show only 4 of the 16 channels.

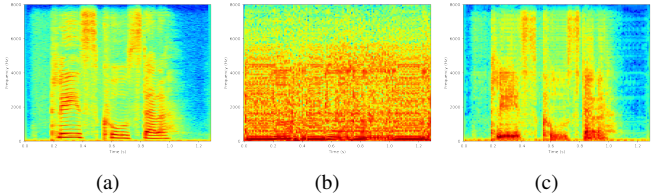


Fig. 3: Spectrograms of (a) original speech, (b) audio when \mathbf{H} has been zeroed out, (c) audio when s and m have been zeroed out.

4.4. Analysis of the speech synthesis process

To investigate how LVC-VC generates audio, we performed spectral analyses of its intermediate representations after each transposed convolutional block. Specifically, we made the model reconstruct a sample utterance and performed STFTs on each channel of the intermediate outputs. Fig. 2 shows the results. In the first stack, we see that the model immediately begins to incorporate content and speaker information from the emergence of voiced segments and the F0 band, respectively. Similar patterns emerge in the subsequent stacks, with the formation of the overall F0 contour and more harmonics. This suggests the gradual addition of more detailed speaker and content information as the signal is upsampled. In addition, individual channels appear to model different aspects of the signal, such as voiced and unvoiced segments, formants, background noise, and silence.

We also investigated how LVC-VC incorporates speaker and content information in the speech synthesis process. To do this, we made the model generate audio with either \mathbf{H} or s and m zeroed out. Fig. 3 shows spectrograms of the resulting output signals. When \mathbf{H} is zeroed out, the F0 and harmonics still form somewhat normally, showing that the speaker’s characteristics have been imparted. However, the spectral envelope and formants do not appear, indicating that no content information is present. Meanwhile, zeroing out s and m gives the opposite result; while the spectral envelope and formants are preserved, the F0 and its harmonics do not form. These results indicate that LVC-VC learns to utilize the speaker and content information in its input features independently, and that it successfully combines this information when generating time-domain audio.

5. CONCLUSION

In this work, we presented LVC-VC, an end-to-end model for zero-shot voice conversion. Rather than disentangling speaker and content information from utterances itself, LVC-VC utilizes a set of input features that already have disentangled content and speaker style information. Using location-variable convolutions, it combines this information within a neural vocoder-like framework, simultaneously performing voice conversion while generating audio. Despite having a compact model size, LVC-VC achieves well-balanced performance that is competitive with or better than several baselines while maintaining intelligibility particularly well. This demonstrates the effectiveness of the model at utilizing and combining the relevant information in the input features for speech synthesis.

6. REFERENCES

- [1] Chin-Cheng Hsu, Hsin-Te Hwang, Yi-Chiao Wu, Yu Tsao, and Hsin-Min Wang, "Voice conversion from unaligned corpora using variational autoencoding wasserstein generative adversarial networks," *arXiv preprint arXiv:1704.00849*, 2017.
- [2] Takuhiro Kaneko, Hirokazu Kameoka, Kou Tanaka, and Nobukatsu Hojo, "CycleGAN-vc2: Improved cycleGAN-based non-parallel voice conversion," in *IEEE International Conference on Acoustics, Speech and Signal Processing (ICASSP)*. IEEE, 2019, pp. 6820–6824.
- [3] Benjamin van Niekirk, Leanne Nortje, and Herman Kamper, "Vector-quantized neural networks for acoustic unit discovery in the zerospeech 2020 challenge," in *Interspeech*, 2020.
- [4] Zhen Zeng, Jianzong Wang, Ning Cheng, and Jing Xiao, "Lvc-net: Efficient condition-dependent modeling network for waveform generation," in *IEEE International Conference on Acoustics, Speech and Signal Processing (ICASSP)*. IEEE, 2021, pp. 6054–6058.
- [5] Kaizhi Qian, Yang Zhang, Shiyu Chang, Xuesong Yang, and Mark Hasegawa-Johnson, "Autovc: Zero-shot voice style transfer with only autoencoder loss," in *International Conference on Machine Learning*. PMLR, 2019, pp. 5210–5219.
- [6] Kaizhi Qian, Zeyu Jin, Mark Hasegawa-Johnson, and Gautham J Mysore, "F0-consistent many-to-many non-parallel voice conversion via conditional autoencoder," in *IEEE International Conference on Acoustics, Speech and Signal Processing (ICASSP)*. IEEE, 2020, pp. 6284–6288.
- [7] Siyang Yuan, Pengyu Cheng, Ruiyi Zhang, Weituo Hao, Zhe Gan, and Lawrence Carin, "Improving zero-shot voice style transfer via disentangled representation learning," in *International Conference on Learning Representations*, 2020.
- [8] Sang-Hoon Lee, Ji-Hoon Kim, Hyunseung Chung, and Seong-Whan Lee, "Voicemixer: Adversarial voice style mixup," *Advances in Neural Information Processing Systems*, vol. 34, 2021.
- [9] Ju-chieh Chou and Hung-Yi Lee, "One-shot voice conversion by separating speaker and content representations with instance normalization," *Interspeech*, pp. 664–668, 2019.
- [10] Yen-Hao Chen, Da-Yi Wu, Tsung-Han Wu, and Hung-yi Lee, "Again-vc: A one-shot voice conversion using activation guidance and adaptive instance normalization," in *IEEE International Conference on Acoustics, Speech and Signal Processing (ICASSP)*. IEEE, 2021, pp. 5954–5958.
- [11] Joan Serrà, Santiago Pascual, and Carlos Segura Perales, "Blow: a single-scale hyperconditioned flow for non-parallel raw-audio voice conversion," *Advances in Neural Information Processing Systems*, vol. 32, pp. 6793–6803, 2019.
- [12] Bac Nguyen and Fabien Cardinaux, "Nvc-net: End-to-end adversarial voice conversion," in *IEEE International Conference on Acoustics, Speech and Signal Processing (ICASSP)*. IEEE, 2022, pp. 7012–7016.
- [13] Anton Kashkin, Ivan Karpukhin, and Svyatoslav Shishkin, "Hifi-vc: High quality asr-based voice conversion," *arXiv preprint arXiv:2203.16937*, 2022.
- [14] Hyeon-Seok Choi, Juheon Lee, Wansoo Kim, Jie Lee, Hoon Heo, and Kyogu Lee, "Neural analysis and synthesis: Reconstructing speech from self-supervised representations," *Advances in Neural Information Processing Systems*, vol. 34, 2021.
- [15] Jungil Kong, Jaehyeon Kim, and Jaekyoung Bae, "Hifi-gan: Generative adversarial networks for efficient and high fidelity speech synthesis," *Advances in Neural Information Processing Systems*, vol. 33, 2020.
- [16] Anmol Gulati et al., "Conformer: Convolution-augmented transformer for speech recognition," in *Interspeech*, 2020, pp. 5036–5040.
- [17] Alexis Conneau, Alexei Baevski, Ronan Collobert, Abdelrahman Mohamed, and Michael Auli, "Unsupervised cross-lingual representation learning for speech recognition," *arXiv preprint arXiv:2006.13979*, 2020.
- [18] Bishnu S Atal and Suzanne L Hanauer, "Speech analysis and synthesis by linear prediction of the speech wave," *The Journal of the Acoustical Society of America*, vol. 50, no. 2B, pp. 637–655, 1971.
- [19] Won Jang, Dan Lim, Jaesam Yoon, Bongwan Kim, and Juntae Kim, "UnivNet: A Neural Vocoder with Multi-Resolution Spectrogram Discriminators for High-Fidelity Waveform Generation," in *Interspeech*, 2021, pp. 2207–2211.
- [20] Joon Son Chung et al., "In defence of metric learning for speaker recognition," in *Interspeech*, 2020, pp. 2977–2981.
- [21] Joon Son Chung, Arsha Nagrani, and Andrew Senior, "Voxceleb2: Deep speaker recognition," in *Interspeech*, 2018, pp. 1086–1090.
- [22] Ryuichi Yamamoto, Eunwoo Song, and Jae-Min Kim, "Parallel wavegan: A fast waveform generation model based on generative adversarial networks with multi-resolution spectrogram," in *IEEE International Conference on Acoustics, Speech and Signal Processing (ICASSP)*. IEEE, 2020, pp. 6199–6203.
- [23] Xudong Mao, Qing Li, Haoran Xie, Raymond YK Lau, Zhen Wang, and Stephen Paul Smolley, "Least squares generative adversarial networks," in *Proceedings of the IEEE International Conference on Computer Vision*, 2017, pp. 2794–2802.
- [24] Junichi Yamagishi, Christophe Veaux, and Kirsten MacDonald, "Cstr vctk corpus: English multi-speaker corpus for cstr voice cloning toolkit (version 0.92)," 2019.
- [25] Ilya Loshchilov and Frank Hutter, "Decoupled weight decay regularization," in *International Conference on Learning Representations*, 2018.
- [26] Mirjam Wester, Zhizheng Wu, and Junichi Yamagishi, "Analysis of the voice conversion challenge 2016 evaluation results," in *Interspeech*, 2016, pp. 1637–1641.
- [27] Alexei Baevski, Yuhao Zhou, Abdelrahman Mohamed, and Michael Auli, "wav2vec 2.0: A framework for self-supervised learning of speech representations," *Advances in Neural Information Processing Systems*, vol. 33, pp. 12449–12460, 2020.
- [28] Thomas Wolf et al., "Transformers: State-of-the-art natural language processing," in *Proceedings of the 2020 Conference on Empirical Methods in Natural Language Processing: System Demonstrations*, 2020, pp. 38–45.
- [29] Hee Soo Heo, Bong-Jin Lee, Jaesung Huh, and Joon Son Chung, "Clova baseline system for the voxceleb speaker recognition challenge 2020," *arXiv preprint arXiv:2009.14153*, 2020.
- [30] Heiga Zen et al., "LibriTTS: A corpus derived from librispeech for text-to-speech," in *Interspeech*, 2019, pp. 1526–1530.

- [31] Gabriel Mittag, Babak Naderi, Assmaa Chehadi, and Sebastian Möller, “Nisqa: A deep cnn-self-attention model for multidimensional speech quality prediction with crowdsourced datasets,” in *Interspeech*, 2021, pp. 2127–2131.
- [32] Alex Krizhevsky, Ilya Sutskever, and Geoffrey E Hinton, “Imagenet classification with deep convolutional neural networks,” *Advances in Neural Information Processing Systems*, vol. 25, 2012.
- [33] Chris Olah, Alexander Mordvintsev, and Ludwig Schubert, “Feature visualization,” *Distill*, vol. 2, no. 11, pp. e7, 2017.
- [34] Tomi Kinnunen, Zhi-Zheng Wu, Kong Aik Lee, Filip Sedlak, Eng Siong Chng, and Haizhou Li, “Vulnerability of speaker verification systems against voice conversion spoofing attacks: The case of telephone speech,” in *IEEE International Conference on Acoustics, Speech and Signal Processing (ICASSP)*. IEEE, 2012, pp. 4401–4404.
- [35] Shivangi Singhal, Rajiv Ratn Shah, Tanmoy Chakraborty, Ponnuram Kumaraguru, and Shin’ichi Satoh, “Spotfake: A multi-modal framework for fake news detection,” in *IEEE Fifth International Conference on Multimedia Big Data (BigMM)*. IEEE, 2019, pp. 39–47.
- [36] Qian Wang, Xiu Lin, Man Zhou, Yanjiao Chen, Cong Wang, Qi Li, and Xiangyang Luo, “Voicepop: A pop noise based anti-spoofing system for voice authentication on smartphones,” in *IEEE Conference on Computer Communications*. IEEE, 2019, pp. 2062–2070.
- [37] Madhu R Kamble, Hardik B Sailor, Hemant A Patil, and Haizhou Li, “Advances in anti-spoofing: from the perspective of asvspoof challenges,” *APSIPA Transactions on Signal and Information Processing*, vol. 9, 2020.
- [38] Hemlata Tak, Jose Patino, Massimiliano Todisco, Andreas Nautsch, Nicholas Evans, and Anthony Larcher, “End-to-end anti-spoofing with rawnet2,” in *IEEE International Conference on Acoustics, Speech and Signal Processing (ICASSP)*. IEEE, 2021, pp. 6369–6373.
- [39] Trisha Mittal, Uttaran Bhattacharya, Rohan Chandra, Aniket Bera, and Dinesh Manocha, “Emotions don’t lie: An audio-visual deepfake detection method using affective cues,” in *Proceedings of the 28th ACM International Conference on Multimedia*, 2020, pp. 2823–2832.
- [40] Hira Dharmyal, Ayesha Ali, Ihsan Ayyub Qazi, and Agha Ali Raza, “Fake audio detection in resource-constrained settings using microfeatures,” *Interspeech*, pp. 4149–4153, 2021.
- [41] Massimiliano Todisco, Xin Wang, Ville Vestman, Md Sahidullah, Héctor Delgado, Andreas Nautsch, Junichi Yamagishi, Nicholas Evans, Tomi Kinnunen, and Kong Aik Lee, “Asvspoof 2019: Future horizons in spoofed and fake audio detection,” *Interspeech*, 2019.
- [42] Junichi Yamagishi et al., “Asvspoof 2021: accelerating progress in spoofed and deepfake speech detection,” in *ASVspoof 2021 Workshop-Automatic Speaker Verification and Spoofing Countermeasures Challenge*, 2021.
- [43] Jiangyan Yi et al., “Add 2022: the first audio deep synthesis detection challenge,” *arXiv preprint arXiv:2202.08433*, 2022.
- [44] Ben Noa Moussa and Eric Urban, “Guidelines for responsible deployment of synthetic voice technology,” <https://docs.microsoft.com/en-us/legal/cognitive-services/speech-service/custom-neural-voice/concepts-guidelines-responsible-deployment-synthetic>, 2022.

A. THEORY BEHIND LOW-QUEFRENCY LIFTERED SPECTROGRAM AS CONTENT FEATURE

In this section, we provide further context on the theory behind using the low-quefrency liftered spectrogram \mathbf{H} as the primary content feature for LVC-VC.

From a signal processing point of view, the physical speech production process can be modeled by a linear system in which the excitation of the vocal cords (the source) is convolved with a representation of the vocal tract (the filter) [18]. Here, the excitation is modeled using either an impulse train (for voiced speech) or white noise (for unvoiced speech), represented by a signal $e(n)$ with Fourier transform $E(z)$. Meanwhile, the vocal tract can be modeled using a discrete time-varying linear filter with impulse response $h(n)$ and transfer function $H(z)$. Therefore, an output speech signal $x(n)$ and its Fourier transform $X(z)$ can be described as follows:

$$x(n) = e(n) * h(n), \quad (1)$$

$$X(z) = E(z)H(z), \quad (2)$$

where $*$ denotes the convolution operation.

At a given point in time, the vocal tract determines the spectral envelope of the voice, which in turn determines the specific phoneme that is produced via formant frequencies. The source-filter model provides a way of modeling the spectral envelope: it can be approximated by the transfer function of the filter, $H(z)$ [18].

We can consider the excitation of the vocal cords $E(z)$ to contain some of the *speaker* information in a spoken utterance. Indeed, $E(z)$ contains information on a voice's fundamental frequency (F0) as well as its harmonic frequencies. Meanwhile, we can consider the spectral envelope and formants $H(z)$ over time to contain a significant portion of the *content* information of an utterance. By separating $H(z)$ from $E(z)$ via deconvolution, we can disentangle the content information an utterance from a large portion of its speaker information. (As we note in the main text of the paper, $H(z)$ still contains some amount of speaker information on its own, which motivates our warping strategy for performing information perturbation during training.)

A.1. Deconvolution in the cepstrum

Recall that a speech signal $x(n)$ can be expressed as a convolution between an excitation signal $e(n)$ and the impulse response of the vocal tract filter $h(n)$ (Eq. 1). In the frequency domain, this convolution becomes equivalent to the multiplication of their respective Fourier transforms (Eq. 2). Taking the logarithms of the absolute values of the Fourier transforms to compute the log magnitude spectra converts the multiplication operation to addition:

$$\log |X(z)| = \log |E(z)H(z)| \quad (3)$$

$$= \log |E(z)| + \log |H(z)|. \quad (4)$$

If we apply a Fourier transform (in practice, actually a discrete cosine transform (DCT) since the log magnitude spectrum only has real components) to the above, we obtain the cepstrum C , which is a frequency distribution of the fluctuations in the curve of the spectrum:

$$C = \text{DCT}(\log |X(z)|) \quad (5)$$

$$= \text{DCT}(\log |E(z)|) + \text{DCT}(\log |H(z)|). \quad (6)$$

If we assume that the source (excitation) spectrum has only rapid fluctuations (since the excitation signal is a stable, regular oscillation), its contribution to the cepstrum will be concentrated in the higher quefrency bins of C . Conversely, the filter (vocal tract) will contribute

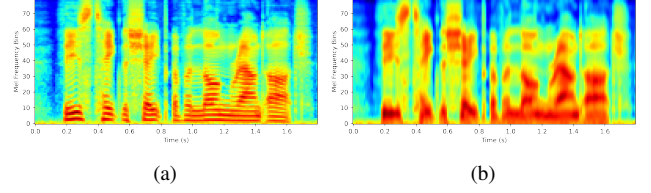


Fig. 4: (a) A sample log-mel spectrogram, and (b) the results of performing low-quefrency liftering on it. Note that (b) captures the spectral envelope and formants of the utterance, but no longer contains information on the F0 and its harmonic frequencies.

slow fluctuations to the spectrum of X and will be concentrated in the lower quefrency bins.

Therefore, the separation of $E(z)$ and $H(z)$ becomes straightforward: we simply have to perform liftering and select the desired quefrency region by multiplying the entire cepstrum by a window at the appropriate position. Low-quefrency liftering, where the quefrency coefficients below a certain point are extracted, allows us to obtain the vocal tract characteristics in the quefrency domain. High-quefrency liftering, the opposite, allows us to obtain the excitation characteristics. Once we have performed liftering, it is a simple matter of performing the inverse DCT to obtain the deconvolved spectral envelope and excitation. Figure 4 illustrates the results of performing low-quefrency liftering on a sample log-mel spectrogram.

B. FURTHER DETAILS ON ANALYSIS OF THE SPEECH SYNTHESIS PROCESS

In this section, we provide additional details about the analyses described in Section 4.4 that were done to further understand the speech synthesis process in LVC-VC.

B.1. Time-domain audio generation

To investigate how LVC-VC generates audio, we performed spectral analyses of the intermediate outputs of the model after each transposed convolutional block. Specifically, we looked at spectrograms of each of these intermediate outputs in order to gain an intuition of what is happening at each step as the model upsamples the input noise sequence to eventually produce the output audio signal.

Recall that LVC-VC starts with an input noise sequence that is at a $\frac{1}{256} \times$ temporal resolution compared to the final output signal. It contains three 1D transposed convolutions that upsample this input sequence by $8 \times$, $8 \times$, and $4 \times$ to produce the final time domain waveform. Therefore, we can essentially consider the outputs of the three transposed convolutional blocks to be downsampled versions of the final output signal with temporal resolutions that are $\frac{1}{32} \times$, $\frac{1}{4} \times$, and $1 \times$ that of real-time. Taking this into account, we computed the STFTs of these downsampled signals using the following Fourier transform parameters:

- $\frac{1}{32} \times$ downsampled signal: 32 point Fourier transform, 32 sample window length, 8 sample hop length, corresponding to audio sampled at 500 Hz.
- $\frac{1}{4} \times$ downsampled signal: 256 point Fourier transform, 256 sample window length, 64 sample hop length, corresponding to audio sampled at 4 kHz.
- $1 \times$ downsampled signal: 1024 point Fourier transform, 1024 sample window length, 256 sample hop length, corresponding to audio sampled at 16 kHz.

Because the model's convolutional layers have 16 channels, the output of each transposed convolutional block also has 16 channels.

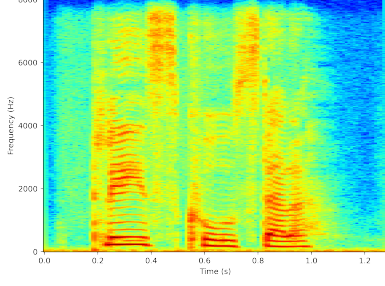


Fig. 5: Spectrogram of the sample utterance that we use to illustrate spectral analyses of the internal representations of LVC-VC.

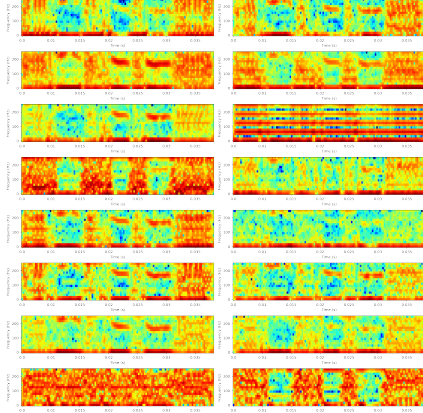


Fig. 6: Results of computing the STFT on the output of the first transposed convolutional stack of LVC-VC. Signals are at a $\frac{1}{32} \times$ temporal resolution compared to real-time.

To demonstrate the results of our experiments, we use a sample utterance from the VCTK corpus to illustrate the results of the spectral analyses we performed on the internal representations of LVC-VC. The utterance is of the phrase “Please call Stella” and is spoken by a female voice. Fig. 5 shows the linear spectrogram of the utterance.

Fig. 6 shows the results of computing the STFT on the 16 channels of the output of the first transposed convolution stack when LVC-VC is tasked with reconstructing the sample utterance. We can see that the model immediately begins to construct content information, as demonstrated by the emergence of three clear voiced segments in the STFT outputs (“Please”, “call”, “Stella”). In these voiced segments, we also see the emergence of the first harmonic band of the speaker’s F0 around the 200 Hz mark. In addition, we can notice that individual channels appear to model different aspects of the audio signal. Some channels appear to model the voiced segments of the utterance, while others appear to model the unvoiced segments, background noise, or silence.

Figs. 7 and 8 show the corresponding STFT visualizations for the outputs of the second and third transposed convolution stacks, respectively. We see that similar patterns emerge in terms of different channels appearing to correspond to different aspects of the final time domain audio signal: voiced segments, unvoiced segments, background noise, and silence. We also see the formation of more harmonic frequencies and the overall F0 contour, indicating the gradual addition of more detailed speaker and content information as the signal propagates and is upsampled through the model.

Overall, these results indicate that the different channels of LVC-

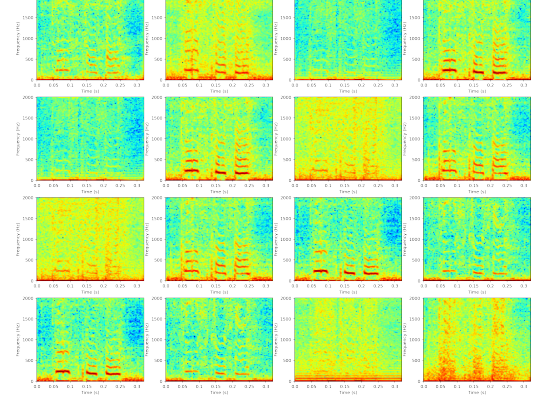


Fig. 7: Results of computing the STFT on the output of the second transposed convolutional stack of LVC-VC. Signals are at a $\frac{1}{4} \times$ temporal resolution compared to real-time.

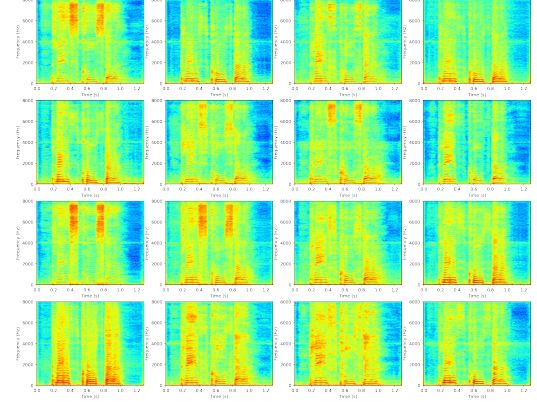


Fig. 8: Results of computing the STFT on the output of the third transposed convolutional stack of LVC-VC. Signals are at the same temporal resolution ($1 \times$) as real-time.

VC’s convolutional layers encode the various aspects of a speech signal, such as voiced and unvoiced segments, vocal cord harmonics, formants, silence, and noise. LVC-VC thus appears to generate audio by starting off with incorporating high-level speaker and content features in the lower layers of the model, and then gradually adding in more fine-grained speaker and content information as it dilates the signal across the time domain and spectrum. These results are perhaps not entirely surprising; we can see them as analogous to the way in which convolutional filters in deep computer vision models learn to encode different aspects of images in their layers, such as edges, colors, and patterns [32, 33].

B.2. Incorporation of speaker and content information

In order to see how LVC-VC incorporates speaker and content information during the audio generation process, we performed experiments where we ablated certain input features and performed spectral analyses of the resulting outputs.

B.2.1. Speaker information

To analyze how LVC-VC incorporates speaker information in the speech generation process, we zeroed out the speaker embedding s and quantized log median F0 m and made the model generate audio using only content features. Then, we performed spectral analyses in

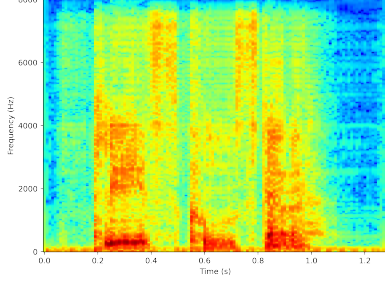


Fig. 9: Spectrogram computed from the signal generated by LVC-VC when s and m have been zeroed out.

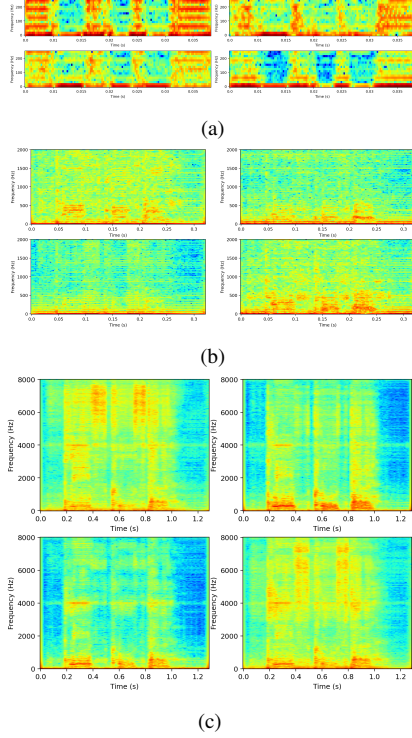


Fig. 10: Results of computing the STFT on the intermediate outputs of LVC-VC after the (a) first, (b) second, and (c) third convolutional stacks when s and m have been zeroed out.

the same way as above by computing the STFTs of the intermediate outputs of the transposed convolution stacks as well as of the final output signal. Fig. 9 illustrates the final output of the model when it generates audio with no speaker information, and Fig. 10 illustrates the intermediate outputs of the transposed convolution stacks. For brevity, we only include visualizations for 4 out of the 16 channels for each of the intermediate outputs.

We see that the spectral envelope and formants of the utterance are well preserved at each intermediate layer and in the final output signal, indicating that the content information has been passed through the model properly. However, we also see that the speaker’s F0 band and its harmonics do not form at any point, indicating that the speaker’s vocal characteristics have not been imparted onto the output signal. Intuitively, this makes sense; since the model does not have any conditioning information about the speaker’s identity, there is no way for it to determine the characteristics of the speaker’s voice. These results demonstrate that the content-related features we feed

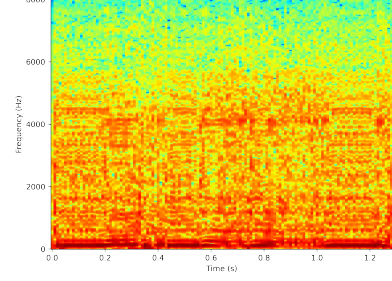


Fig. 11: Spectrogram computed from the signal generated by LVC-VC when \mathbf{H} has been zeroed out.

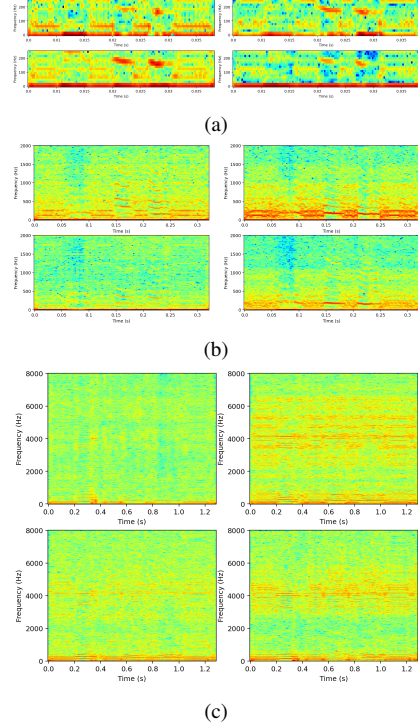


Fig. 12: Results of computing the STFT on the intermediate outputs of LVC-VC after the (a) first, (b) second, and (c) third convolutional stacks when \mathbf{H} has been zeroed out.

into LVC-VC properly transfer the content information of the source utterance to the output of the model without allowing any speaker information through.

B.2.2. Content information.

To analyze how LVC-VC incorporates content information, we made it generate audio after zeroing out the low-frequency lifted mel spectrogram \mathbf{H} . However, we did continue to provide the normalized F0 contour \mathbf{p}_{norm} in order to see how it would interact with the speaker information in s and m . Fig. 11 illustrates the final output of the model when it generates audio with no content information, and Fig. 12 illustrates the intermediate outputs of the transposed convolution stacks.

The outputs are essentially the reverse of what we see when we zero out the speaker information. Voiced segments, which are specified by the normalized F0 contour \mathbf{p}_{norm} , still appear to be

generated more or less properly. The shape and contour of the F0 and its harmonic frequencies still form somewhat normally, demonstrating that \mathbf{p}_{norm} is being successfully “un-normalized” by combining it with the speaker information. However, as expected, the spectral envelope and formants do not form at all, resulting in a situation in which the F0 contour is present but there is no content information for it to correspond to. In addition, we see that in the absence of the knowledge of which unvoiced frames are silent, the model appears to fill in the gaps with white noise-like artifacts up to around 6,000 Hz (as seen in Figure 11). These results indicate that the speaker-related features that are fed into LVC-VC allow the model to effectively express the speaker’s vocal characteristics in the output audio without passing any content information through.

B.2.3. Summary

Overall, the results support the following intuition: LVC-VC combines speaker information with the content features in such a way that “un-warps” the low-quefreny liftered spectrogram \mathbf{H} and “un-normalizes” the normalized F0 contour \mathbf{p}_{norm} . This indicates that our strategy for LVC-VC’s design—combining carefully designed input features in an end-to-end vocoder-like framework, rather than training the model to explicitly disentangle and recombine the information in an utterance—is an effective way of synthesizing audio using the speaker and content information taken from different utterances.

C. FULL RESULTS OF ABLATION STUDIES ON LVC-VC

Table 3: Seen-to-seen voice conversion evaluation results for various ablations of LVC-VC.

Model	WER	CER	EER	NISQA
LVC-VC	22.69	9.55	18.50	4.00 ± 0.08
w/o GMM embeddings	23.33	10.18	15.50	3.86 ± 0.09
w/o SSC loss	15.79	5.97	68.00	4.16 ± 0.08
w/o warping \mathbf{H}	19.80	8.51	41.50	3.96 ± 0.09
w/o \mathbf{p}_{norm}	23.11	10.22	18.50	3.71 ± 0.10
w/o m	22.34	9.05	21.00	3.91 ± 0.09

Table 4: Unseen-to-seen voice conversion evaluation results for various ablations of LVC-VC.

Model	WER	CER	EER	NISQA
LVC-VC	17.37	7.03	20.00	3.89 ± 0.14
w/o GMM embeddings	16.64	7.10	16.25	3.69 ± 0.15
w/o SSC loss	12.25	4.38	71.25	4.04 ± 0.13
w/o warping \mathbf{H}	19.56	8.40	42.50	3.81 ± 0.17
w/o \mathbf{p}_{norm}	19.01	7.61	25.00	3.66 ± 0.15
w/o m	18.28	7.46	20.00	3.82 ± 0.13

Table 5: Unseen-to-unseen voice conversion evaluation results for various ablations of LVC-VC.

Model	WER	CER	EER	NISQA
LVC-VC	20.10	8.29	26.25	3.50 ± 0.13
w/o GMM embeddings	26.92	11.11	25.00	2.89 ± 0.14
w/o SSC loss	16.78	6.64	68.75	3.83 ± 0.13
w/o warping \mathbf{H}	19.76	7.39	51.25	3.62 ± 0.17
w/o \mathbf{p}_{norm}	21.33	8.60	32.50	3.36 ± 0.18
w/o m	22.90	9.90	28.75	3.47 ± 0.14

D. ETHICAL CONSIDERATIONS

Voice conversion is a field that is unfortunately fraught with potential misuse. “Audio deepfakes” can be used to deceive people by synthetically generating speech and attributing them to certain individuals; this can lead to problems such as voice spoofing [34] or the spread of fake news and misinformation [35]. To the extent that this work enables more realistic manipulation of speaker identities, it could potentially exacerbate these misuses if used by a malicious party.

A wide variety of work has sought to address these issues by developing techniques for anti-spoofing [36, 37, 38] and general fake audio detection [39, 40]. Recently, there have also been several public challenges to encourage the development of systems that can detect fake audio [41, 42, 43]. Going forward, the speech machine learning community should continue to encourage these research directions and raise awareness of the potential problems with high-fidelity synthetic audio.

There are also approaches that can be taken from a more immediately practical standpoint [44]. First, organizations that utilize synthetic voices generated by text-to-speech (TTS) or voice conversion technologies should provide adequate disclosure to audiences when they do so; this is especially important if using the voice of a well-known person. Doing this can help minimize the risk of harmful outcomes from potential deception and can also increase trust in the organization delivering the voice. When generating or converting voices to sound like real speakers, the owners of the voices should also have control over their voice model (i.e., give permission for how and where it will be used) and be compensated for their use if appropriate.